THE ASTROPHYSICAL JOURNAL, 469:L93–L96, 1996 October 1

TIDAL DISRUPTION AND TAILS FROM THE CARINA DWARF SPHEROIDAL GALAXY

J. R. KUHN[1]
National Solar Observatory/Sacramento Peak, National Optical Astronomy Observatories, P.O. Box 62, Sunspot, NM 88349; and Michigan State University, Department of Physics and Astronomy

AND

HORACE A. SMITH AND SUZANNE L. HAWLEY[2]
Michigan State University, Department of Physics and Astronomy, East Lansing, MI 48824 USA
Received 1996 April 25; accepted 1996 April 25

ABSTRACT

New photometry of regions beyond the classical tidal radius of Carina exposes a Carina-like stellar distribution that is about 1% of the central surface density and which extends at least as far as 2° (3.5 kpc) from Carina's center. The detections of a spatially extended RR Lyrae distribution, and a significant Carina-like stellar population at large central distances confirm predictions of the time-dependent tidal interaction model and suggest that Carina is not in virial equilibrium.

Subject headings: dark matter — galaxies: individual (Carina) — galaxies: Local Group — galaxies: structure — Galaxy: kinematics and dynamics

1. INTRODUCTION

The Local Group dwarf spheroidal (dS) galaxy Carina has a range of interesting dynamical and stellar properties (e.g., Mighell 1990; Smecker-Hane et al. 1996). In particular, the Carina stellar velocity dispersion is often interpreted as evidence of a large mass-to-light ratio ($M/L = 39$; cf. Mateo et al. 1993). In contrast, dynamical calculations (Kuhn & Miller 1989, hereafter KM89) showed that the time-dependent tidal interaction of a dS with the Milky Way (MW) could significantly inflate its stellar velocity dispersion above the virial equilibrium value. Thus, Carina's apparent high M/L ratio and interesting star formation history make it an important target to examine for evidence of MW tidal interactions.

The argument that a dS could be "heated" by its MW interaction, even when its core radius is significantly smaller than the classical tidal radius, has been controversial. Despite evidence of extra-tidal stars in Sculptor (Innanen & Papp 1979), the discovery of a tidally disrupted dwarf spheroidal in Sagittarius (Ibata, Gilmore, & Irwin 1994), the apparent discovery of extratidal stellar "debris" near Sextans (Gould et al. 1992), and the detection of extratidal stars near several dS galaxies (Irwin & Hatzidimitriou 1995, hereafter IH95), Pryor (1996) recently argued that none of the dS systems except for Sagittarius are likely to have been significantly affected by the MW.

Kuhn (1993) suggested that a distinguishing feature of the KM89 model is that dS systems which have been tidally heated should exhibit "tails" that extend several tidal radii (r_t) from their centers and trace their orbits. These tails are long-lived and, depending on the form of the distant MW potential, may persist for several orbital periods. The observation of such extra-tidal remnants might allow the determination of the dS orbit and the MW mass within large galactocentric distances. It is interesting that corresponding tidal tails from globular clusters (at much lower relative surface densities) have recently been observed by Grillmair et al. (1995).

Unambiguous observations of the extratidal surface density are critical to understanding the dynamics of dS galaxies. The KM89 calculations implied that the extratidal stellar mass could be as large or larger than the central mass in a long-lived but near-resonance dS system. In this model, the dS has experienced repeated perigalacticon passages which inflate its central M/L ratio and generate a co-moving tidal tail. In contrast, Oh, Lin, & Aarseth (1995) could not generate surface density enhancements above 10^{-4} at radii larger than r_t without catastrophic tidal disruption of the stellar system. Piatek & Pryor (1995) reached a similar conclusion, but their calculations only traced a stellar system through one perigalacticon passage. Neither of these calculations considered the time-dependent tidal regime of the KM89 calculations. The observational situation has recently improved beyond the Demers, Beland, & Kunkel (1983) Carina observations, which implied an upper limit of 4% for the relative surface density beyond 16′ from the center: IH95 included Carina in their survey of several dS and found evidence for extratidal stars out to 40′ from the center. Both of these measurements were based on star counts and were difficult because of the large galactic "background" at Carina's Galactic latitude ($b = -22°$).

Photographic observations of Carina by Saha et al. (1986, hereafter SMS86) showed that it has a number of RR Lyraes (although not nearly as many as the Sculptor, Ursa Minor, or Draco dwarf galaxies). One approach to finding distant tidal debris is to look for these variable stars at the distance of Carina in a wide-field survey. Another approach is to adopt a color-magnitude ($c - m$) diagram of Carina as a statistical template to "count stars." This $c - m$ selection technique allows the detection of a Carina stellar population to a much lower surface density than is otherwise possible using simple star counts. Results from both techniques are described here.

2. DATA AND RESULTS

The observations and further analysis will be described in more detail elsewhere—here we summarize the most important features of the data and the results. Observations were obtained from a completely photometric run during 1996

[1] Visiting astronomer, Cerro Tololo Inter-American Observatory.
[2] NSF Young Investigator.

February 15–18 at Cerro Tololo Inter-American Observatory, using a 2 K × 2 K pixel CCD at the f/7.5 focus of the 1.5 m telescope. The image scale was 0.″43 pixel^{-1}, yielding a field of view 15′ square. Eleven fields were observed, nine along the major axis (including a field near the Carina center) and two along the minor axis. The major axis fields were on centers spaced approximately 0.°5 apart, arranged in a nearly symmetric pattern around the Carina center so that the two outermost fields were approximately 2° east and west of the center. The minor axis fields (located approximately north and south of Carina) were 1° from the center. Fields were shifted by as much as 10′ from the nominal symmetrical displacement pattern to avoid bright foreground stars. Between seven and 11 V-band epochs and three or four I-band epochs were obtained for each field, and one B-band epoch was obtained for the central field. The V and I photometry for each epoch was obtained from a pair of 4 minute observations, while the B photometry was obtained from a pair of 8 minute exposures. The FWHM of the stellar profiles was typically 3–4 pixels.

CCD images were bias-subtracted and flat-fielded with dome flats, using standard IRAF procedures. Aperture photometry was obtained using the IRAF Daophotx software package with aperture radii of 1 and 4 pixels. Stars in each field were selected from a master image that was generated by spatially shifting and co-adding all images of the same field and color. The threshold for finding stars was chosen to detect objects at limiting V and I magnitudes about 2 mag fainter than the Carina horizontal branch.

The measured extinction coefficients from each night were consistent and all nights were photometric. The standard calibration was performed using nightly observations of Landolt (1992) standards. The measurement uncertainties in our aperture corrections, color terms and atmospheric extinction result in a total calibration uncertainty compared to the standard system of ±0.03 mag. Figure 1 shows our V, $V - I$ color-magnitude diagrams for the central Carina field and the 1° north displaced field (the "background" reference). Photometry was obtained for a total of approximately 35,000 objects from all fields. Comparable and fainter photometry for the central region of Carina, consistent with our 0.03 mag calibration uncertainty, is described by Smecker-Hane et al. (1994, 1996).

2.1. *RR Lyrae Results*

We devised a search algorithm for RR Lyraes by first identifying all stars within one V magnitude interval centered on the Carina horizontal branch (HB). The $V - I$ color of the candidate stars was also restricted to a 1 mag interval which included the HB. From the ~10 epochs of V-band photometry measurements in each field, we selected stars with a standard deviation (σ_V) greater than 0.15 mag. The average standard deviation for all stars in this magnitude interval was 0.04 mag. We compared photometry from both the small and large radius apertures to rule out variability resulting from blended stellar images or atmospheric seeing changes. In the central field there were seven variable stars detected. All of these stars were previously identified by SMS86 as variables and four had light curve solutions. Monte Carlo experiments (consistent with our ~10 epoch time domain) suggest that for less than 50% of our sample will we be able to derive a light curve period with an error less than 5%. Thus we are unlikely to improve on the 20 epoch period determinations of Saha et al., and a full light curve analysis of our variables awaits further observations.

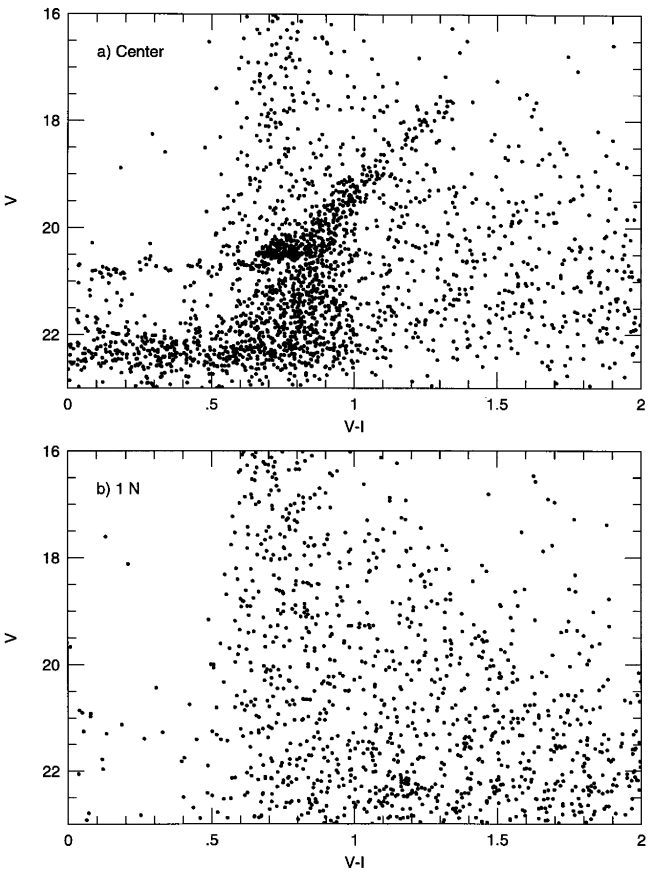

FIG. 1.—Color-magnitude diagrams for the 15′ × 15′ fields: (*a*) near the center of Carina, (*b*) 1° north along the minor axis (background reference field).

It is somewhat unsettling that SMS86 identified a total of 31 variable "candidates" in our central field, where we detected seven RR Lyrae stars. However, we note that SMS86 could find light curve solutions for only eight of their candidates, all eight of which they found to be RR Lyrae stars. Four of the seven stars we confirm as variable are among the eight for which SMS86 obtained light curves. The remaining four stars for which SMS86 obtained light curves have σ_V below our threshold. Some of the SMS86 candidates may not be variable on a short timescale. Others may in fact be RR Lyraes not clearly identified as such by these selection criteria. Note that our variable star detection criteria were deliberately chosen to trade a high detection efficiency for a low false detection rate. To check this we looked for variable stars in $c - m$ "space" redward of $V - I = 1$. As expected, none were found, and we believe our false RR Lyrae detection rate is insignificant. Although we require more observing epochs to measure the precise RR Lyrae detection efficiency, given the comparison with the SMS86 light curve variables, we estimate our efficiency to be about 50%. Monte Carlo estimates of σ_V, using observing intervals comparable to these data and assuming an ab-type RR Lyrae light curve, imply that a variability threshold of 0.15 mag should reveal about 80% of the ab types. Fortunately our results do not depend on the value of the detection efficiency, only on the fact that the false detection rate is low, and that the detection efficiency is not greater in the offset fields than in the central field.

TABLE 1

RR Lyrae Stars in the Central and 0.°5 E Offset Fields

R. A. (2000)	Decl. (2000)	r_{cen} [a]	σ_V (mag)	V	$V-I$	SMS86 (Light Curve) ID
6:44:44.6.....	−50:54:55	27.9	0.22	20.724	0.45	...
6:43:49.3.....	−50:48:02	21.8	0.24	20.757	0.57	...
6:43:48.8.....	−50:47:55	21.8	0.18	20.764	0.69	...
6:43:28.7.....	−50:55:45	16.0	0.19	20.705	0.53	4 (L)
6:40:29.4.....	−51:00:16	12.5	0.17	20.910	0.50	151
6:40:38.4.....	−51:01:37	11.4	0.16	20.819	0.49	142
6:40:39.3.....	−50:55:59	11.4	0.20	20.781	0.64	141
6:40:37.2.....	−50:59:23	11.3	0.18	20.710	0.42	144 (L)
6:40:52.3.....	−50:58:55	9.0	0.27	20.697	0.46	126 (L)
6:40:53.3.....	−50:58:52	9.0	0.35	20.718	0.63	125 (L)
6:41:05.6.....	−51:00:26	7.0	0.23	20.727	0.43	116 (L)

[a] In arcminutes.

Applying this procedure to all 11 fields reveals four variables in the field centered 0.°41 to the east of Carina's center, and none in any of the other offset fields. The coordinates, magnitude, color, variability (σ_V), and projected distance (r_{cen}) from the nominal Carina center ($6^h40^m.4$, −50°55′ [1950]; Cannon, Hawarden, & Tritton 1977) is given for all 11 RR Lyrae detections in Table 1. The RR Lyraes we detected in the central field are also listed along with their SMS86 identification and a notation if Saha et al. obtained a light curve solution. Note that the mean V magnitude of our offset east field RR Lyraes is 20.74 ± 0.03, in good agreement with the mean brightness (20.71 ± 0.01) we measure for the SMS86 light curve variables detected in the (distinct) central field. Although none of the variables lie beyond 28′, the relative RR Lyrae surface density in the east field (centered 25′ from the center) is significantly higher than expected given Carina's classical tidal radius of 28.′8 (cf. IH95). We detected no variables in the west offset observations, although the nearest west field was centered 40′ from Carina's center. Unfortunately, only the nearest east offset field sampled the density distribution near the classical tidal radius. We integrated a classical truncated King profile that fits the Demers et al. (1983) surface density measurements over the spatial geometry of our central and offset fields. If the variables are distributed like this average stellar surface density then the ratio of the number of variables in the two fields should be 90:1 (i.e., there should be 360 in the central field). The IH95 density measurements similarly imply that we should see 12 times more variables in the near-central field than the offset field. Our observation of seven central and four offset variables is difficult to reconcile with the hypothesis that even the more extended IH95 density model describes the RR Lyrae data. The alternative that our RR Lyrae detection algorithm is 6–12 times less efficient in the near-central field than in the offset field is untenable.

We also confirm the new Smecker-Hane et al. distance modulus for Carina. Using the same galactic extinction ($A_V = 0.08$) and RR Lyrae absolute magnitude ($M_V = 0.45 \pm 0.07$) they used, we obtain a distance modulus for Carina of 20.18 ± 0.08 mag, consistent with their measurement of 20.12 ± 0.08.

2.2. *Color-Magnitude Diagram Results*

From the $c - m$ data of Figure 1, we note that there are roughly 1000 Carina stars brighter than $V = 21.5$ in the central field. The young red horizontal branch clump alone contains about 200 stars. The total MW disk and halo statistical background also contains about 1000 stars, distributed more uniformly at least to the red of the old disk/halo turnoff. Since most of the Carina stars are restricted to the HB (young and old) and the giant branch, a sensitive technique for measuring a Carina surface density at 1% or less of the central density involves fitting $c - m$ "templates." We define the $c - m$ templates as including all measured stars in a given field, regardless of whether they are Carina stars or background stars.

On the basis of the KM89 model we expect few, if any, Carina stars in regions perpendicular to the long axis (since the major axis defines the Carina orbital plane). Thus we make the assumption (which is tested below) that the $c - m$ diagram of the fields 1° to the north and south fairly measure the "background." This background, $B(c, m)$, can be treated as a smooth function of the $V - I$ color, c, and V magnitude, v. We then construct a Carina reference function by subtracting $B(c, m)$ from the $c - m$ function observed in the central field. The remainder describes the Carina stars, and we label this $C(c, m)$. A good estimate of the density of Carina and background stars in an arbitrary field with an observed $c - m$ function, $D(c, m)$, is then found by projecting D onto the functions B and C. In practice, these functions were estimated by binning the $c - m$ data in 0.5 V-magnitude bins between 16 and 21.5, and 0.1 mag $V - I$ bins between −0.25 and 2.75. The functions were also determined using V magnitude bins of 0.25 mag and $V - I$ bins of 0.05 mag. Results were also checked by changing the faint-end limiting magnitude of the $c - m$ diagram used in the fitting procedure and by picking different fields for the reference background function. All of these tests yielded results that are consistent with the data plotted in Figure 2.

To project D onto B and C, we minimize the expression $\sum_{c,m}\{D(c, m) - aC(c, m) - bB(c, m)\}^2$ with respect to the least-squares parameters a and b, and where the sum extends over the V and $V - I$ magnitude domain. Now a, as formulated, describes the density of Carina stars in the arbitrary field (in units of the central field density) and b gives the density of "background" stars, which should be approximately 1. We include the variable b in the fit to account for foreground stellar surface density variations between fields. To estimate the statistical, and some systematic, uncertainties in the derived a and b parameters, each field was divided into quadrants and the parameters were separately determined for each quadrant. The standard deviation from these four samples in each field was adopted as the density uncertainty that defines the error flags in Figure 2. Note that physical surface density gradients across each field will inflate these error estimates.

Figure 2 shows the mean surface density of $c - m$ selected

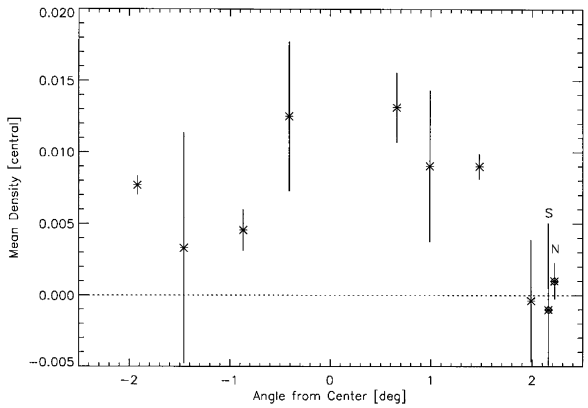

FIG. 2.—The surface density distribution of Carina-like stars derived from color-magnitude least-squares fitting. The density is expressed in units of Carina's central surface density. The points (*diamonds*) labeled "N" and "S" show the north and south minor axis results. Points plotted at negative angles are for fields to the east of Carina, positive angles show fields to the west (along the major axis).

Carina stars in each field as a function of distance from Carina's center. The density has been obtained by scaling the mean a coefficient from each field (which is computed in units of the actual displaced-center Carina $c - m$ data) by the ratio of the mean central density in our actual near-central field, to the "true" density at the dS center point. This factor of 0.23 was calculated as the ratio of the integral of the IH95 density function over our actual $15' \times 15'$ central field position, to the integral of the (constant) central IH95 density over a $15' \times 15'$ field.

We actually measure the surface density *excess* of Carina stars with respect to the "background" field using this technique. Since the background field might also have a small Carina surface density, we are, in effect, setting the surface density zero point by defining the function B. For example, choosing a background field other than the north, south, or 2° west fields results in negative surface density estimates for these fields. While we cannot rule out a small positive offset in our zeropoint, it is clear that the minor axis observations have the lowest surface density of the 9 fields. The density excess in the major axis fields is clearly significant except for the 1°.5 east (which is only marginally significant) and the 2° west observations. We note that our Carina near-center density measurements are consistent with the IH95 measurements.

3. DISCUSSION

The $c - m$ analysis shows a population of Carina stars with a surface density of nearly 1% of the central density far beyond the classical tidal radius and in both directions along the major axis. Although this new technique obtains the Carina density excess with respect to a specific background field, the consistency of our surface density measurements in the minor axis fields suggests that Carina is not extended perpendicular to its major axis. The radial density distribution is poorly sampled by our nine fields, but it is also apparently "clumpy" (or nonmonotonic as IH95 observed) and not well described by a power law.

We did not detect variables beyond the classical tidal radius, but based on the central RR Lyrae density and our $c - m$ extratidal density measurements, extratidal RR Lyraes are quite sparse and should not have been found. On the other hand, we do see a large surface density of variables *near* the tidal radius that is difficult to reconcile with other surface density measurements (e.g., IH95). It appears that the RR Lyrae distribution is more extended (or "clumpier") than the distribution implied by the majority of the Carina stars. Improving the RR Lyrae statistics is an important future observing priority. Smecker-Hane et al. (1994) found no evidence for such segregation, but they observed only the center of what we should consider to be a much larger stellar system. It appears that the old RR Lyrae population is distributed differently than the $c - m$ population we trace in Figure 2.

We believe the case for a significant extratidal stellar population in the vicinity of at least one of the dS galaxies is compelling. Our results for Carina confirm the IH95 star count data near the tidal radius, while providing strong evidence for tidal debris at even larger dS distances. Our innermost fields show a surface density of about 1% of the Carina central density, consistent with the outermost IH95 measurements, while our data from larger distances indicate a surface density excess that extends at least 2° from the center of Carina in the east direction.

It is perhaps surprising that such a large fraction of the mass of Carina lies outside its tidal radius. Our data imply that at least 25% of Carina's luminous mass is between 0°.5 and 2° from its center. Can the central core of Carina be in virial equilibrium? None of the dynamical equilibrium, or near-equilibrium, model calculations yield the large surface densities that we see beyond Carina's tidal radius. In contrast, the KM89 nonequilibrium tidal interaction model naturally predicts both an inflated central M/L ratio and an extratidal surface density as large as a few percent of the central density.

H. A. S. acknowledges support from NSF grant AST93-17403. S. L. H. was partially supported by NSF Young Investigator award AST94-57455.

REFERENCES

Cannon, R. D., Hawarden, T. G., & Tritton, S. B. 1977, MNRAS, 180, 81P
Demers, S., Beland, S., & Kunkel, W. E. 1983, PASP, 95, 354
Gould, A., Guhathakurta, R., Richstone, D., & Flynn, C. 1992, ApJ, 388, 345
Grillmair, C. J., Freeman, K. C., Irwin, M., & Quinn, P. J. 1995, AJ, 109, 2553
Ibata, R. A., Gilmore, G., & Irwin, M. J. 1994, Nature, 370, 194
Innanen, K. A., & Papp, K. A. 1979, AJ, 84, 601
Irwin, M., & Hatzidimitriou, D. 1995, MNRAS, 277, 1354 (IH95)
Kuhn, J. R. 1993, ApJ, 409, L13
Kuhn, J. R., & Miller, R. H. 1989, ApJ, 341, L41 (KM89)
Landolt, A. U. 1992, AJ, 104, 340
Mateo, M., Olszewski, E., Pryor, C., Welch, D., & Fischer, P. 1993, AJ, 105, 510
Mighell, K. J. 1990, A&A, 82, 1
Oh, K. S., Lin, D., & Aarseth, S. J. 1995, ApJ, 442, 142
Piatek, S., & Pryor, C. 1995, AJ, 109, 1071
Pryor, C. 1996, ASP Conf. Ser., Vol. 424, Formation of the Galactic Halo—Inside and Out, ed. H. Morrison & A. Sarajedini (San Francisco: ASP) 424
Saha, A., Monet, D. G., & Seitzer, P. 1986, AJ, 92, 302 (SMS86)
Smecker-Hane, T. A., Stetson, P. B., Hesser, J. E., & Lehnert, M. D. 1994, AJ, 108, 507
Smecker-Hane, T. A., Stetson, P. B., Hesser, J. E., & VandenBerg, D. A. 1996, From Stars to Galaxies: The Impact of Stellar Physics on Galaxy Evolution, ed. C. Leitherer, U. Fritze-van Alvensleben, & J. Huchra (San Francisco: ASP), in press